Enhancing quantum field theory simulations on NISQ devices with Hamiltonian truncation

James Ingoldby,[*] Michael Spannowsky,[†] Timur Sypchenko,[‡] and Simon Williams[§]
Institute for Particle Physics Phenomenology, Durham University, Durham DH1 3LE, United Kingdom

(Received 20 August 2024; accepted 18 October 2024; published 19 November 2024)

Quantum computers can efficiently simulate highly entangled quantum systems, offering a solution to challenges facing classical simulation of quantum field theories (QFTs). This paper presents an alternative to traditional methods for simulating the real-time evolution in QFTs by leveraging Hamiltonian truncation (HT). As a use case, we study the Schwinger model, systematically reducing the complexity of the Hamiltonian via HT while preserving essential physical properties. For the observables studied in this paper, the HT approach converges quickly with the number of qubits, allowing for the interesting physics processes to be captured without needing many qubits. Identifying the truncated free Hamiltonian's eigenbasis with the quantum device's computational basis avoids the need for complicated and costly state preparation routines, reducing the algorithm's overall circuit depth and required coherence time. As a result, the HT approach to simulating QFTs on a quantum device is well suited to noisy-intermediate scale quantum devices, which have a limited number of qubits and short coherence times. We validate our approach by running simulations on a noisy-intermediate scale quantum device, showcasing strong agreement with theoretical predictions. We highlight the potential of HT for simulating QFTs on quantum hardware.

DOI: 10.1103/PhysRevD.110.096016

I. INTRODUCTION

The simulation of quantum field theories (QFTs) is crucial for understanding fundamental particles and their interactions and forms the cornerstone of modern particle theory. Despite their success, simulating QFTs on classical computers is difficult, and contemporary approaches suffer from challenges which severely limit the exploration of QFTs, such as the so-called sign problem, which is a fundamental difficulty in Monte Carlo importance sampling algorithms [1–3]. These challenges are especially pronounced in areas such as quantum chromodynamics (QCD) at finite density and nonperturbative calculations of the real-time dynamics of hadrons.

Quantum computers have the ability to simulate the real-time dynamics of highly entangled systems, therefore offering a solution to the sign problem and providing a natural regime for simulating QFTs. As a result, there has been great interest in designing algorithms for the simulation of QFTs on quantum devices [4–10], with most approaches choosing to adopt the Kogut-Susskind Hamiltonian formulation for SU(N) lattice gauge theory [11]. The lattice approach, whilst powerful, has its own set of limitations. One of the most prominent problems facing this approach is the initial-state preparation, achieved by preparing specific quantum states on the device using state-preparation routines. These routines are known to be extremely costly, and the resources required to implement the state-preparation for an arbitrary state can scale exponentially [12–15].

This paper presents an alternative method that leverages Hamiltonian truncation (HT) techniques to facilitate the nonperturbative, real-time simulation of QFTs on a quantum device. It will be shown that this approach allows for the Hamiltonian to be constructed such that complicated and costly state-preparation routines are not needed to simulate the time evolution of a QFT. Furthermore, for the observables studied in this paper, it will be shown that the HT approach converges quickly as the truncation increases, thus allowing for the system's dynamics to be captured reliably without needing many qubits. As a result, the HT approach has a reduced circuit depth on fewer qubits, making the method well suited for noisy-intermediate scale quantum (NISQ) devices, which have limited numbers of qubits and short coherence times.

Hamiltonian truncation is a nonperturbative numerical method for approximating the spectrum and dynamics of strongly coupled quantum systems. In this approach, the

[*]Contact author: james.a.ingoldby@durham.ac.uk
[†]Contact author: michael.spannowsky@durham.ac.uk
[‡]Contact author: timur.sypchenko@durham.ac.uk
[§]Contact author: simon.j.williams@durham.ac.uk

Hamiltonian is expressed on a truncated basis of states. It is particularly useful when applied to QFTs because selecting a finite number of basis states reduces the infinite-dimensional Hamiltonian of a QFT to a finite-dimensional one, making computational analysis possible. Furthermore, HT can be applied directly to continuum QFT Hamiltonians without discretizing them first on a lattice, removing the need to control systematic uncertainties arising from lattice artifacts. This formalism, which is an alternative to the lattice, has enabled the study of a wide variety of phenomena, including critical points in scalar field theories [16–21], scattering processes [22–24], and the decay of metastable vacua [25,26]. For a general introduction and review of applications, see Refs. [27,28].

Truncation schemes have also been extensively developed within the context of lattice Hamiltonians. In these schemes, there are local Hilbert spaces for the lattice sites or links, and each local Hilbert space gets truncated independently. Such schemes can also be applied to non-Abelian gauge theories and to those in higher dimensions, for example in [29–33]. Truncation schemes which act on operators have been considered in [34]. See Refs. [35,36] for an overview.

To explore and illustrate the efficacy of the HT approach and its suitability to NISQ devices, we consider the massive Schwinger model [37–39], which is analogous to quantum electrodynamics in $(1+1)$ dimensions. The model provides a simple yet rich framework to test the quantum simulation of QFTs via HT. The Schwinger model is exactly solvable in its massless form and offers insights into phenomena such as confinement and screening, which are crucial for understanding more complex theories like QCD.

In Sec. II, the HT procedure is outlined by first bosonizing the model, which reexpresses it as an interacting scalar field theory and removes all the gauge redundant degrees of freedom. This scalar field theory is constructed on the finite-volume circle before applying HT, without introducing a lattice. The process of truncating the Hilbert space reduces the complexity of the Hamiltonian whilst ensuring that it retains the essential features and interactions to simulate real-time evolution accurately. Consequently, the truncated Hamiltonian is more suited to implementation on NISQ devices with limited qubits and coherence times.

In Sec. III, we demonstrate this suitability by considering the dynamics of the model after a quench and evaluating time-evolution using different truncation levels. We see that the model gives a good description of the postquench dynamics of the Schwinger model, even with a small number of resources, ultimately allowing for the model to be run on the `ibm_brisbane` quantum computer. Utilizing the control and error suppression techniques provided by Q-CTRL [40,41] to improve the fidelity of the results, we obtain the first simulation of a QFT on a quantum device through HT. The results show a remarkably accurate simulation of the postquench dynamics of the Schwinger model on a NISQ device.

This work highlights the potential of HT for simulating QFTs on near-term quantum hardware, achieving accurate and precise results with low resource costs. Furthermore, it paves the way for future research in leveraging quantum devices for nonperturbative field theory simulations.

II. HAMILTONIAN TRUNCATION

HT [27,28] involves approximating the full Hamiltonian of a theory by restricting it to a finite subspace of the Hilbert space. This technique is particularly useful when perturbative methods fail, such as in strongly coupled systems or when nonperturbative effects are significant.

In this approach, the first step is to decompose the Hamiltonian of the quantum system of interest into a solvable part H_0, plus an interaction V so that

$$H = H_0 + V. \tag{2.1}$$

The eigenstates and corresponding eigenvalues of the solvable part can then be identified and labelled $H_0|i\rangle = E_i|i\rangle$. Next, a truncation scheme is introduced. An energy cutoff, denoted as $E_{\max}$, is applied, and we retain only states with H_0 eigenvalues up to this cutoff $E_i \leq E_{\max}$ in the truncated Hilbert space. To the extent that low-energy states in the full theory lie within this truncated Hilbert space, the low energy physics of the full theory will be well approximated in HT.

The truncated Hamiltonian is then represented as a matrix, which acts on states of a truncated basis. Numerical diagonalization can then yield approximate eigenvalues and eigenvectors for the system. The eigenvalues correspond to the approximate energy levels, while the eigenvectors provide information about the corresponding quantum states.

The results are then analyzed, checking the convergence with respect to the cutoff $E_{\max}$. This involves increasing $E_{\max}$ and stabilizing physical observables such as energy levels or correlation functions. The physical interpretation of these results is then made in the original problem's context, often compared with known analytical results or experimental data if available.

In the QFT context, truncation of the basis acts as a kind of nonlocal UV regularization,[1] so that in a QFT with UV divergences, there will be observables that diverge as $E_{\max}$ is increased. In this case, nonlocal counterterms must be added to the Hamiltonian to renormalize the theory. A systematic procedure for constructing the nonlocal terms is outlined in Refs. [42,43]. Even in UV finite QFTs, many

[1]The regularization is nonlocal because the cutoff $E_{\max}$ acts on the total energy of a state and does not take into account how widely separated in space different particles or excitations in the same state are.

observables converge in a power like fashion (i.e. as $O \sim O_\infty + c/E_{\max}^p$ for a model-dependent positive power p) as the cutoff is increased, and it can be beneficial to add improvement terms to the Hamiltonian which improve the rate of convergence [16–20,44–46]. These terms are constructed to account for states above the HT cutoff on low energy dynamics, and are analogous to higher dimension effective operators included in the action of a low-energy effective field theory.

Hamiltonian truncation is a versatile technique adaptable to various quantum systems and field theories. It has the potential to bridge the gap between exact analytical solutions and purely numerical approaches like lattice field theory, offering a tool for studying complex quantum phenomena.

A. Hamiltonian truncation applied to the Schwinger model

The Schwinger model has become a benchmark scenario for comparing nonperturbative methods in simulating field theories, ranging from lattice gauge theories [47–51] over Hamiltonian simulation with tensor networks [52–56] to its simulation on quantum devices in various quantum computing paradigms [57–64].

The Schwinger model has also been investigated using truncated light cone Hamiltonians [65–67]. The light cone Hamiltonian generates translations in the light cone coordinate $x^+ = (t + x)/\sqrt{2}$. An overview of light cone quantization is given in Ref. [68] and the application of quantum computing to QFTs defined using the truncated light cone Hamiltonian approach has been investigated in [69].

The massive Schwinger model is quantum electrodynamics in $(1 + 1)$ dimensions describing the dynamics of fermions and photons. The Lagrangian takes the usual form,

$$\mathcal{L} = -\frac{1}{4} F_{\mu\nu} F^{\mu\nu} + \bar{\psi}(i\partial\!\!\!/ - gA\!\!\!/ - m)\psi, \tag{2.2}$$

where $F_{\mu\nu} \equiv \partial_\mu A_\nu - \partial_\nu A_\mu$ is the electromagnetic field tensor, A_μ is a U(1) photon field, ψ is a two-component fermion field, and g is the coupling strength with dimensions of mass. In $(1 + 1)$ dimensions, there are no directions transverse to the momenta of moving particles. Therefore, there are no propagating photon degrees of freedom.

To begin, we consider the massless case by setting $m = 0$, such that the massless Schwinger model Lagrangian takes the form

$$\mathcal{L}_0 = -\frac{1}{4} F_{\mu\nu} F^{\mu\nu} + \bar{\psi}(i\partial\!\!\!/ - gA\!\!\!/)\psi. \tag{2.3}$$

In this limit, the model has an anomalous U(1) chiral symmetry, and the θ term can be removed with a chiral transformation. The massless Schwinger model was solved exactly by Schwinger [37], who showed that the model's Green's functions were those of a free massive scalar field. Therefore, it is possible to reformulate the model as a massive scalar field theory, with the Hamiltonian density [70]

$$\mathcal{H}_0 = \frac{1}{2} :\Pi^2 + (\partial_x \phi)^2 + \frac{g^2}{\pi}\phi^2: \ , \tag{2.4}$$

where $::$ denotes the normal ordering of the creation and annihilation operators used to represent the scalar field, changing the definitions of these operators, and therefore the normal ordering convention only adds an extra constant to $\mathcal{H}_0$. The mass can be read off as $M^2 \equiv g^2/\pi$, and Π is the canonical momentum of the scalar field ϕ. This reformulation of the model is an example of bosonization [39,71]. Although the Schwinger model can be bosonized, this is not the case for generic gauge theories. However, the HT approach can still be applied in these cases by taking H_0 to be a solvable theory other than the free scalar field. See the discussion in Ref. [28].

In this study, we are interested in simulating the real-time evolution of interacting quantum field theories. Therefore, we will consider the massive Schwinger model from Eq. (2.2). The mass m breaks chiral symmetry, rendering the θ term physical. The background electric field strength is related to θ through $E_B = g\theta/2\pi$ [38].

Adding the fermion mass introduces a interaction term to the bosonized Hamiltonian [70], such that

$$\mathcal{H} = \mathcal{H}_0 - 2cmM :\cos(\sqrt{4\pi}\phi + \theta):, \tag{2.5}$$

where $\mathcal{H}_0$ is the free theory Hamiltonian from Eq. (2.4), and c depends on the definition of the creation and annihilation operators which are to be normal ordered [71].

We consider the massive Schwinger model placed on a finite circle of length L (which ensures that the spectrum is discrete). On the circle, gauge fields must satisfy periodic boundary conditions, but fermion fields can satisfy $\psi(t, x) = e^{i\delta}\psi(t, x + L)$. Since δ can be changed using a type of gauge transformation [72], physical quantities should not depend on this choice. After bosonization, the scalar field then satisfies periodic boundary conditions.

To employ Hamiltonian truncation directly to the bosonized theory (without lattice discretization), we decompose the Hamiltonian as in Eq. (2.1) and take as the solvable part to be

$$H_0 = \int_0^L dx \mathcal{H}_0 = \sum_{n=-\infty}^{\infty} E_n \, a_n^\dagger a_n, \tag{2.6}$$

where we identify the momentum $k_n = (2\pi n/L)$ for $n \in \mathbb{Z}$ and the energy $E_n = \sqrt{k_n^2 + M^2}$ of the nth mode. The commutation relations for the creation and annihilation

operators take the usual form: $[a_n, a_m] = [a_n^\dagger, a_m^\dagger] = 0$ and $[a_n, a_m^\dagger] = \delta_{n,m}$.

The truncated basis we use is formed from the eigenstates of Eq. (2.6), which are Fock states that take the form

$$|\{\mathbf{r}\}\rangle = \prod_{n=-\infty}^{n=\infty} \frac{1}{\sqrt{r_n!}} (a_n^\dagger)^{r_n} |0\rangle, \tag{2.7}$$

where $|0\rangle$ is the vacuum state satisfying $a_n|0\rangle = 0$ for all modes n.

The interaction is the integral of the second term in Eq. (2.5)

$$V = -cmM \int_0^L dx : \exp\left[i\sqrt{4\pi}\phi(x) + i\theta\right] : + \text{H.c.}, \tag{2.8}$$

where on the finite volume circle, the scalar field ϕ entering Eq. (2.8) should be understood as the following sum over modes

$$\phi(x) = \sum_{n=-\infty}^{\infty} \frac{1}{\sqrt{2LE_n}} (a_n e^{ik_n x} + a_n^\dagger e^{-ik_n x}). \tag{2.9}$$

The sum runs over all integer mode numbers n, including the zero modes $n = 0$ (see [55] and references therein).

We use the dots : : in (2.8) to represent normal ordering with respect to the bosonic creation and annihilation operators of Eqs. (2.6) and (2.9). For simplicity, we take the coefficient c to equal its infinite volume limiting value

$$c = \frac{e^\gamma}{4\pi}, \tag{2.10}$$

where $\gamma \approx 0.57721$ is the Euler-Mascheroni constant.

Using Eq. (2.9), the normal-ordered exponential can be expanded in terms of the creation and annihilation operators

$$\begin{aligned} : \exp\left[i\sqrt{4\pi}\phi(x)\right] : &\coloneqq \prod_{n=-\infty}^{\infty} \exp\left[\sqrt{\frac{2\pi}{LE_n}} i e^{-ik_n x} a_n^\dagger\right] \exp\left[\sqrt{\frac{2\pi}{LE_n}} i e^{ik_n x} a_n\right], \\ &= \prod_{n=-\infty}^{\infty} \sum_{j_n, j_n'=0}^{\infty} \frac{1}{j_n'! j_n!} \left(i\sqrt{\frac{2\pi}{LE_n}}\right)^{j_n + j_n'} e^{ik_n x(j_n - j_n')} (a_n^\dagger)^{j_n'} (a_n)^{j_n}. \end{aligned} \tag{2.11}$$

The matrix elements of the interaction V between basis states can then be calculated by combining Eqs. (2.7), (2.8), and (2.11). The result is

$$\begin{aligned} \langle\{\mathbf{r}'\}|V|\{\mathbf{r}\}\rangle = -cm_f ML e^{i\theta} \delta_{r_0', r_0} \prod_{n=-\infty}^{\infty} \frac{1}{\sqrt{r_n'! r_n!}} \sum_{j_n, j_n'=0} \frac{1}{j_n'! j_n!} \left(i\sqrt{\frac{2\pi}{LE_n}}\right)^{j_n + j_n'} \\ \times \langle 0|(a_n)^{r_n'} (a_n^\dagger)^{j_n'} (a_n)^{j_n} (a_n^\dagger)^{r_n} |0\rangle + \text{H.c.}, \end{aligned} \tag{2.12}$$

where the product of the creation and annihilation operators is given by [73]

$$\langle 0|(a_n)^{r_n'} (a_n^\dagger)^{j_n'} (a_n)^{j_n} (a_n^\dagger)^{r_n} |0\rangle = \binom{r_n'}{j_n'} \binom{r_n}{j_n} j_n'! j_n! (r_n - j_n)! \delta_{r_n' - j_n', r_n - j_n} \Theta(r_n - j_n). \tag{2.13}$$

The integral over space in Eq. (2.8) imposes momentum conservation as an additional constraint. As a result, the matrix element in Eq. (2.12) vanishes unless

$$\sum_{n=-\infty}^{\infty} n(r_n - r_n') = 0, \tag{2.14}$$

where we have used the delta function in Eq. (2.13) to eliminate the $j_n^{(\prime)}$ indices in favor of the occupation numbers $r_n^{(\prime)}$. In this paper, we will consider only states with vanishing total momentum.

The final step is to build the Hamiltonian as an explicit matrix in the basis of Fock states, defined in Eq. (2.7), with eigenvalues of H_0 less than, or equal to E_{max}. It has been explicitly shown that, for QFTs defined as conformal field theories deformed with relevant operators on a cylinder space-time, the number of basis states grows exponentially with the value of the energy cutoff, E_{max} [16,74]. Therefore, the size of the Hamiltonian will grow exponentially with the truncation, quickly rendering the real-time evolution of a QFT intractable on a classical device. A qubit-based quantum computer's exponentially growing Hilbert space allows for efficient information encoding. Therefore, if the

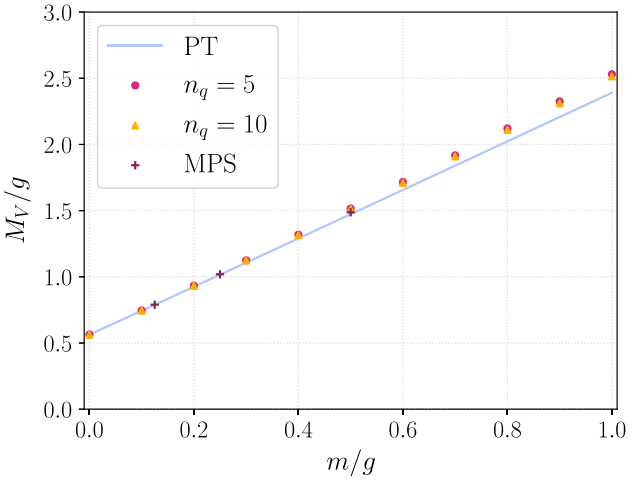

FIG. 1. Comparison of the vector mass, M_V, for varying fermion masses, m. The HT model shows good agreement with perturbation theory (PT) in the quantity m/g [75] to second order, and with matrix product state (MPS) results taken from [52].

size of the Hamiltonian grows exponentially with $E_{\max}$, then the scaling of the number of required qubits will grow at most polynomially.

For the analysis presented in this paper, we will only take $\theta = 0$, in which case the Schwinger model has two additional discrete symmetries: parity (P) and charge conjugation (C). In the bosonized theory, the action of C is to send $\phi(x,t) \to -\phi(x,t)$, and P sends $\phi(x,t) \to -\phi(-x,t)$. We therefore divide our truncated Hilbert space into four subsectors of states which are even or odd under the two symmetries, and construct separate smaller truncated Hamiltonians in the relevant subsectors, thus simplifying our analysis.

For quantum computing applications, it is convenient to redefine the cutoff of the truncated Hilbert space using the number of qubits, n_q, required to represent time evolution using the Hamiltonian (within a particular symmetry subsector). To do this, we order the relevant states in energy and take the first 2^{n_q} as our truncated basis, such that the Hamiltonian has the size $(2^{n_q} \times 2^{n_q})$.

To test our framework, we first consider the value of the vector mass in the Schwinger model, at different fermion mass values. This mass is simply the difference in energy between the lowest energy states in the C even P even, and the C odd P odd subsectors. Figure 1 shows a comparison of the vector mass calculated using the HT approach compared with calculations from second order perturbation theory [75] and matrix product states [52]. To construct the HT calculation we choose the volume $(gL) = 8$. Since finite volume effects are exponentially suppressed for $M_V L \gg 1$ [76], we expect finite volume effects to be small with this choice.

In Fig. 1, we see that the HT method is well converged even for small truncation values, agreeing well with both perturbative and nonperturbative methods at small fermion masses with a truncation of $n_q = 5$. The comparisons between HT and the two infinite-volume methods also confirm that finite volume effects are small for $(gL) = 8$. We see exact agreement between all methods at a value of $(m/g) = 0.2$, and this value will be used in Sec. III when simulating the time evolution of the system on a quantum device.

We note that while energy differences between states are well converged, the ground state energy diverges as $\sim m^2 \log E_{\max}$, just like the free massless fermion theory when perturbed with a mass term in $(1+1)$D. Divergences that affect individual state energies but not energy differences do not affect time evolution, or the determination of particle masses and can be renormalized away in HT by introducing an effective Hamiltonian [42,43].

III. TRUNCATED SCHWINGER MODEL ON A QUANTUM DEVICE

In the Hamiltonian framework, the real-time evolution of the quantum system,

$$U(t) = e^{-iHt}, \tag{3.1}$$

can be naturally implemented on a quantum device by using a product formula method based on the Trotter-Suzuki decomposition [77–79]. Consider a Hamiltonian expressed as a sum of noncommuting operators, $H = \sum_i H_i$. The time-evolution operator, $U(t)$, can be approximated by

$$\mathcal{U}(t) = \left[\prod_i e^{-iH_i t/n}\right]^n, \tag{3.2}$$

up to an error $\mathcal{O}(t^2/n)$, where n is a positive integer. The operator $\mathcal{U}(t)$ defines the Trotterized time evolution, which divides the total evolution time, t, into n steps of time $\delta t = t/n$. The total time evolution is therefore achieved by iteratively applying n so-called Trotter steps, such that the Trotterized time evolution is exact in the limit $n \to \infty$.

In this section, we demonstrate how the Trotterization method can be used to simulate the real-time evolution of the Schwinger model constructed from the HT approach on a quantum device. We test the model's suitability for NISQ devices by evaluating the algorithm's performance at different truncations and ultimately running the simulation on the `ibm_brisbane` quantum computer, which operates a 127-qubit Eagle R3 processor.

A. Time evolution via quantum simulation

To efficiently simulate the time evolution of a QFT on a quantum device, the Hamiltonian of the model must first be mapped onto a basis corresponding to operations native to the quantum device. For a qubit-based quantum computer, such as the `ibm_brisbane` device used for this paper, a

suitable basis of operations is constructed from tensor products of the Pauli operators and an identity operator, $(\sigma_0, \sigma_1, \sigma_2, \sigma_3)$, such that

$$H = \sum_{i_1,\ldots,i_{n_q}=0}^{3} \alpha_{i_1,\ldots,i_{n_q}} (\sigma_{i_1} \otimes \cdots \otimes \sigma_{i_{n_q}}), \tag{3.3}$$

where $\alpha_{i_1,\ldots,i_{n_q}}$ is the coefficient of the corresponding Pauli term, $(\sigma_{i_1} \otimes \cdots \otimes \sigma_{i_{n_q}})$. The exponentials of Pauli terms can be implemented on a qubit-based quantum device through a sequence of single-qubit rotation gates and CNOT gates. A circuit can then be constructed for a single Trotter step of the time evolution by calculating the form of Eq. (3.2). The number of qubits required and the circuit depth for a single Trotter step will grow with the size of Hamiltonian. The time evolution of the QFT is then simulated on a quantum device by following three steps: (1) prepare the initial state, (2) apply the Trotter step circuit iteratively for n-Trotter steps, and (3) measure the circuit with respect to an observable.

Preparing the initial state is a highly nontrivial task and has been shown to require exponential circuit depths to construct arbitrary quantum states without ancillary qubits [12]. Using ancillary qubits, the circuit depth scaling can be reduced to polynomial scaling at the cost of an exponentially growing number of ancillary qubits [13–15]. The final step in the time evolution also requires a state-preparation circuit to rotate the system into a basis such that the desired observable can be measured. Therefore, the circuit depth can grow very rapidly due to the state preparation schemes that need to be implemented, and this has been identified as one of the limiting factors of implementing lattice models on a NISQ device.

In contrast, the HT method allows for the Hamiltonian to be constructed such that the ground state of the free theory, H_0, corresponds exactly to the ground state of the qubit-based quantum device, namely the zeroth state in the computational basis. As a result, complicated and costly state-preparation routines are not required to prepare the ground state of the system. This approach, therefore, offers an advantage over lattice models for simulating QFTs on NISQ devices by reducing the circuit depth requirements for time evolution.

The size of the Hamiltonian, and by extension, the number of qubits required to implement the time evolution, of the Schwinger model obtained from HT is determined by the cutoff energy, $E_{\max}$, and the volume, L. In this paper, we will vary the cutoff energy only, setting the volume, $(gL) = 8$, at a large enough value to approximate the theory well. From Eq. (2.4), the scalar mass is $M = g/\sqrt{\pi}$. The Hilbert space is bosonic and is constructed from the eigenbasis of the free Hamiltonian in Eq. (2.4). As a result, it is not trivial to represent the operators within the Hamiltonian in terms of the fermion creation and annihilation operators. Thus, the massive Schwinger model Hamiltonian from Eq. (2.5) cannot be easily decomposed into tensor products of Pauli operators, which are natural operations for qubit based devices. For this model, this may be a limiting factor for the HT approach as the number of qubits increases because Pauli decomposition leads to an exponentially growing number of Pauli terms in the decomposition of the Hamiltonian. New techniques in the construction of the Hilbert space may be needed to achieve the true potential of this approach. In this paper, it will be shown that systems with small numbers of qubits are sufficient to describe the dynamics of the model and that the approach is well suited to NISQ devices.

An interesting process to study is the postquench dynamics of the Schwinger model. A quench is achieved by preparing the system in the ground state of the free theory, H_0, and then instantaneously "switching on" the potential term, V, such that the system now evolves under the total Hamiltonian, $H = H_0 + V$. For the Schwinger model presented in Sec. II, this is equivalent to switching on the fermion mass, m. To describe this process, we only need to construct and use the Hamiltonian in the C even, P even subsector, since our initial state lies in this subsector, and the C and P symmetries prevent time evolution to states outside this subsector. The state of the system after postquench evolution is, therefore,

$$|\psi(t)\rangle = e^{-iHt}|\psi(0)\rangle \approx \left[\prod_i e^{-iH_i t/n}\right]^n |\psi(0)\rangle. \tag{3.4}$$

The dynamics of the model can then be examined by establishing the probability that the system is in the ground state of the free, $m = 0$ theory. We define the time-dependent observable $G(t)$, such that

$$G(t) = \langle \mathrm{vac}|e^{-iHt}|\mathrm{vac}\rangle, \tag{3.5}$$

where the ground state of the free Hamiltonian is defined as $|\mathrm{vac}\rangle = |0\rangle$ in the computational basis of the qubit device. We will examine the time dependence of $|G(t)|^2$, and explore the effects of truncation and Trotterization errors on this probability, and investigate the feasibility of simulating the model on NISQ devices.

It is important to quantify the error introduced by the truncation by comparing the accuracy of the time-evolution calculation at different truncations. In practice, the task is to achieve a trade-off between the resources required to simulate the model and the truncation error, minimizing both as much as possible. Figure 2 shows one period of the time-evolution of the quenched system from Eq. (2.5) with $(m/g) = 0.2$ for different truncations. Here, the time evolution has been calculated by brute-force exponentiation of the Hamiltonian using a scaling and squaring algorithm [80] available through NumPy [81]. From now on, we will call this method the *Exp*-method. This method simulates the

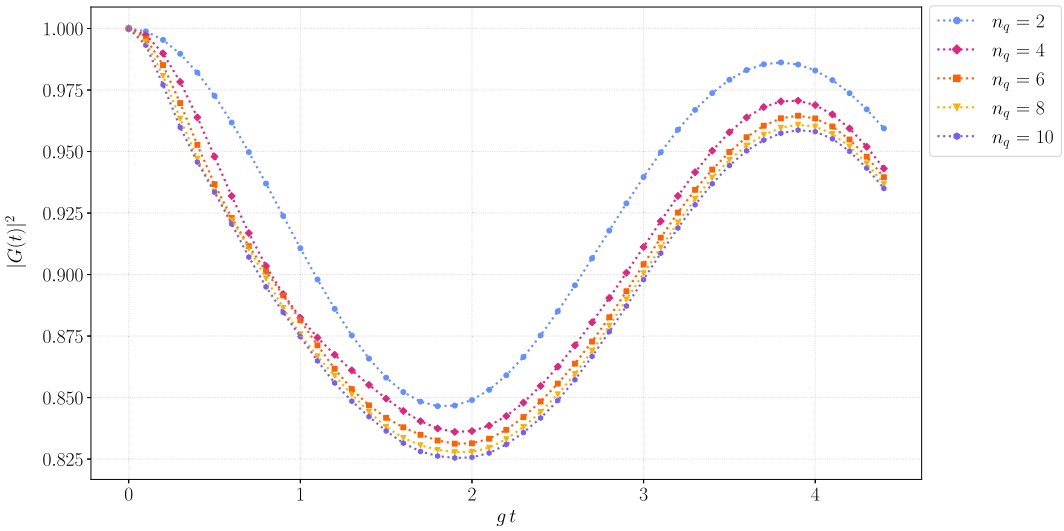

FIG. 2. Comparison of the time evolution of the Schwinger model at different truncations with $(m/g) = 0.2$. The time evolution has been calculated by the *Exp*-method: brute-force exponentiation of the Hamiltonian. The HT method shows quick convergence as the truncation increases, allowing for the dynamics to be reliably captured using only a small number of qubits.

time evolution without Trotterization errors. The model exhibits good convergence as the truncation increases and performs remarkably well for small truncations, describing the postquench dynamics well. The good convergence we see validates our parameter choice $(m/g) = 0.2$.

Together with the truncation, another significant source of error is the so-called Trotter error arising from approximating the time evolution operator from Eq. (3.2). This study will use first-order Trotterization, which approximates the time evolution up to an error $\mathcal{O}(t^2/n)$. Therefore, to minimize the error induced by Trotterization, one must split the time evolution into sufficiently small time steps, δt. However, performing many Trotter steps increases the resource cost of simulating the time evolution, specifically increasing the required circuit depth for quantum simulations. Therefore, again, there is a trade-off between choosing a small enough Trotter step and the resources used. Figure 3 shows the time evolution of the Schwinger model for different values of $(g\delta t)$ compared to the Exp-method. The simulations have been executed with a truncation of $n_q = 2$ and $n_q = 6$, as shown by the blue and yellow lines in Fig. 3, respectively. The Trotterized time-evolution has been performed using the BaseSampler quantum simulator from Qiskit [82], which simulates a fully fault-tolerant quantum device. We see that the model is remarkably resilient to Trotter error and that the time evolution with $(g\delta t) = 0.1$

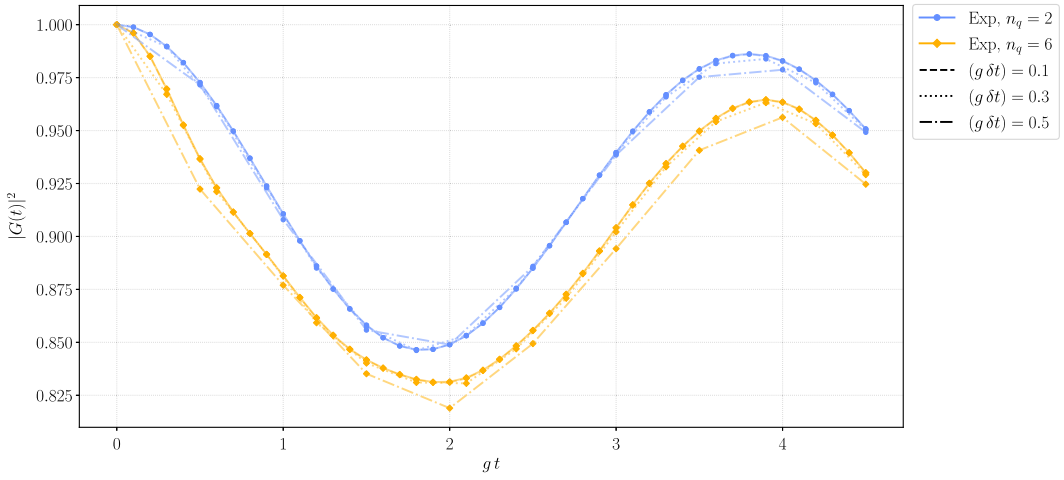

FIG. 3. Time evolution of the Schwinger model with varying Trotter time steps compared to the brute-force exponentiation of the Hamiltonian, so-called Exp. The Trotterized time evolution was performed on a quantum simulator that simulates a fully fault-tolerant quantum device for truncations of $n_q = 2$ (blue) and $n_q = 6$ (yellow). The system exhibits increasing Trotter errors when taking more time steps.

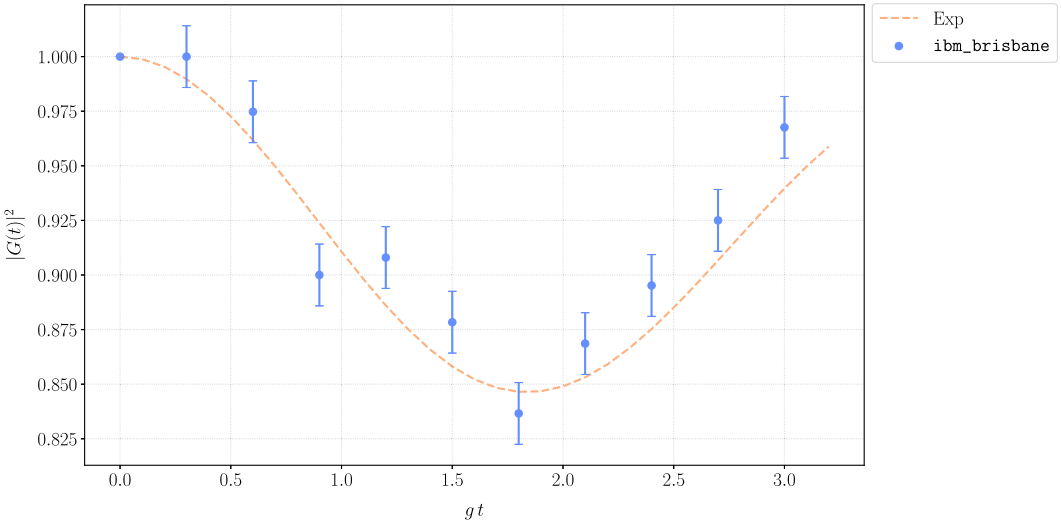

FIG. 4. Time evolution of the Schwinger model via HT run on the `ibm_brisbane` 127-qubit quantum computer. The results have been enhanced using error mitigation and suppression routines through Qiskit [82] and Q-CTRL [40,41]. The output of the quantum device agrees well with the brute-force exponentiation of the Hamiltonian, Exp, achieving a $\chi^2/\text{d.o.f.} = 1.63$. This remarkable agreement demonstrates the suitability of the HT approach to the simulation of QFTs on NISQ devices.

agrees exactly with the Exp-method, even at larger evolution times. However, as the Trotter step increases, the error is more pronounced at large evolution times. This indicates a Trotter error, which grows cumulatively with each Trotter step. As the time step is increased to $(g\delta t) = 0.5$, it is clear that the Trotter error increases, and the distribution deviates away from the Exp-method more quickly for both cases.

Mitigating theoretical errors whilst also remaining within realistic resource constraints of NISQ devices is a challenge for all quantum computing approaches to simulating QFTs. From Fig. 2, we see that the HT method allows for good convergence without needing many qubits. Similarly, we see in Fig. 3 that the time evolution of the Schwinger model via HT does not suffer greatly from Trotter error, even for relatively large Trotter time steps. For this reason, quantum simulation via HT is potentially well suited to NISQ devices, which have few qubits and short decoherence times.

B. Schwinger model on NISQ devices

To determine the feasibility of using the HT approach to simulating QFTs on a quantum device, the time evolution of the Schwinger model has been run on the `ibm_brisbane` quantum computer, a 127-qubit device with an Eagle R3 quantum processor. The model has been constructed to use minimal resources whilst retaining the interesting dynamics of the postquench system. Therefore, the Hamiltonian from Eq. (2.5) has been truncated to run on $n_q = 2$ qubits with a $(m/g) = 0.2$ coupling. A Trotter time step of $(g\delta t) = 0.3$ has been chosen to limit the algorithm's circuit depth and mitigate decoherence. To further suppress the errors from the quantum computer, the AI-driven error suppression pipeline Q-CTRL [40,41,83] has been used through the Qiskit platform [82].

Figure 4 presents the results from the quantum computer compared to the Exp-method. Each data point has been generated from 5000 shots on the quantum computer, and the statistical errors are displayed. The agreement between the distributions from the quantum computer and the Exp-method have been quantified with a $\chi^2/\text{d.o.f.} = 1.63$. The quantum device's performance is remarkable, showing good agreement with the Exp-method. These results highlight the suitability of the HT approach to quantum simulation for NISQ devices. With the interesting physics of the Schwinger model's postquench dynamics being captured using only a small number of qubits, and without the need for complicated and costly state preparation, HT provides a promising route towards simulating the time evolution of QFTs on near-term quantum devices.

IV. CONCLUSION

This study demonstrates the viability of using HT techniques to facilitate the nonperturbative, real-time simulation of QFTs on NISQ devices. By focusing on the Schwinger model, a $(1+1)$-dimensional quantum electrodynamics system, we have showcased our approach's practicality and benefits.

Our findings indicate that HT significantly reduces the complexity of the problem by removing the need for complicated and costly state preparation routines, reducing the overall circuit depth of the algorithm. Furthermore, for the observables studied in this paper, we have shown that the HT approach converges quickly, thus capturing the dynamics of the system without requiring many qubits.

Combined, these attributes of HT make it feasible to implement on NISQ devices, which have limited qubits and coherence times.

We demonstrate the suitability of the HT approach for NISQ devices by running a time-evolution algorithm on the `ibm_brisbane` quantum computer using only two qubits. We employed the Trotter-Suzuki decomposition to approximate the time-evolution operator, facilitating the implementation of real-time dynamics on the quantum device. Our results show good agreement with the classical brute-force exponentiation of the Hamiltonian, the Exp-method, achieving a $\chi^2/\text{d.o.f.} = 1.63$, even when executed on hardware with inherent noise and operational constraints, as shown in Fig. 4. Despite the small number qubits, the system gives a good qualitative description of the underlying physics.

In conclusion, our work highlights the potential of HT as a viable pathway for simulating QFTs on quantum hardware. It encourages more complex simulations and offers a scalable and efficient approach for leveraging quantum devices in nonperturbative field theory research. Future work will extend this approach to more complex models and explore its applicability to a broader range of quantum simulations.

ACKNOWLEDGMENTS

We acknowledge the use of IBM Quantum services for this work.

The views expressed are those of the authors, and do not reflect the official policy or position of IBM or the IBM Quantum team.

[1] H. De Raedt and A. Lagendijk, Monte Carlo calculation of the thermodynamic properties of a quantum model: A one-dimensional fermion lattice model, Phys. Rev. Lett. **46**, 77 (1981).
[2] W. von der Linden, A quantum Monte Carlo approach to many-body physics, Phys. Rep. **220**, 53 (1992).
[3] T. D. Kieu and C. J. Griffin, Monte Carlo simulations with indefinite and complex-valued measures, Phys. Rev. E **49**, 3855 (1994).
[4] M. C. Bañuls *et al.*, Simulating lattice gauge theories within quantum technologies, Eur. Phys. J. D **74**, 165 (2020).
[5] S. P. Jordan, K. S. M. Lee, and J. Preskill, Quantum computation of scattering in scalar quantum field theories, Quantum Inf. Comput. **14**, 1014 (2014).
[6] S. P. Jordan, K. S. M. Lee, and J. Preskill, Quantum algorithms for quantum field theories, Science **336**, 1130 (2012).
[7] S. P. Jordan, K. S. M. Lee, and J. Preskill, Quantum algorithms for fermionic quantum field theories, arXiv:1404.7115.
[8] J. Y. Araz, S. Schenk, and M. Spannowsky, Toward a quantum simulation of nonlinear sigma models with a topological term, Phys. Rev. A **107**, 032619 (2023).
[9] M. Fromm, O. Philipsen, M. Spannowsky, and C. Winterowd, Simulating Z_2 lattice gauge theory with the variational quantum thermalizer, Eur. Phys. J. Quantum Technol. **11**, 20 (2024).
[10] S. Abel, M. Spannowsky, and S. Williams, Simulating quantum field theories on continuous-variable quantum computers, Phys. Rev. A **110**, 012607 (2024).
[11] J. Kogut and L. Susskind, Hamiltonian formulation of Wilson's lattice gauge theories, Phys. Rev. D **11**, 395 (1975).
[12] X. Sun, G. Tian, S. Yang, P. Yuan, and S. Zhang, Asymptotically optimal circuit depth for quantum state preparation and general unitary synthesis, IEEE Trans. Comput.-Aided Des. Integr. Circuits Syst. **42**, 3301 (2023).
[13] M. Plesch and I. C. V. Brukner, Quantum-state preparation with universal gate decompositions, Phys. Rev. A **83**, 032302 (2011).
[14] X.-M. Zhang, M.-H. Yung, and X. Yuan, Low-depth quantum state preparation, Phys. Rev. Res. **3**, 043200 (2021).
[15] X.-M. Zhang, T. Li, and X. Yuan, Quantum state preparation with optimal circuit depth: Implementations and applications, Phys. Rev. Lett. **129**, 230504 (2022).
[16] M. Hogervorst, S. Rychkov, and B. C. van Rees, Truncated conformal space approach in d dimensions: A cheap alternative to lattice field theory?, Phys. Rev. D **91**, 025005 (2015).
[17] S. Rychkov and L. G. Vitale, Hamiltonian truncation study of the ϕ^4 theory in two dimensions, Phys. Rev. D **91**, 085011 (2015).
[18] S. Rychkov and L. G. Vitale, Hamiltonian truncation study of the ϕ^4 theory in two dimensions. II. The $\mathbb{Z}_2$ -broken phase and the Chang duality, Phys. Rev. D **93**, 065014 (2016).
[19] J. Elias-Miro, S. Rychkov, and L. G. Vitale, High-precision calculations in strongly coupled quantum field theory with next-to-leading-order renormalized Hamiltonian truncation, J. High Energy Phys. 10 (2017) 213.
[20] J. Elias-Miro, S. Rychkov, and L. G. Vitale, NLO renormalization in the Hamiltonian truncation, Phys. Rev. D **96**, 065024 (2017).
[21] N. Anand, E. Katz, Z. U. Khandker, and M. T. Walters, Nonperturbative dynamics of $(2+1)$d ϕ^4-theory from Hamiltonian truncation, J. High Energy Phys. 05 (2021) 190.
[22] Z. Bajnok and M. Lajer, Truncated Hilbert space approach to the 2d ϕ^4 theory, J. High Energy Phys. 10 (2016) 050.
[23] B. Gabai and X. Yin, On the S-matrix of Ising field theory in two dimensions, J. High Energy Phys. 10 (2022) 168.

[24] B. Henning, H. Murayama, F. Riva, J. O. Thompson, and M. T. Walters, Towards a nonperturbative construction of the *S*-matrix, J. High Energy Phys. 05 (2023) 197.

[25] D. Szász-Schagrin and G. Takács, False vacuum decay in the $(1+1)$-dimensional φ^4 theory, Phys. Rev. D **106**, 025008 (2022).

[26] M. Lencsés, G. Mussardo, and G. Takács, Variations on vacuum decay: The scaling Ising and tricritical Ising field theories, Phys. Rev. D **106**, 105003 (2022).

[27] A. J. A. James, R. M. Konik, P. Lecheminant, N. J. Robinson, and A. M. Tsvelik, Non-perturbative methodologies for low-dimensional strongly-correlated systems: From non-Abelian bosonization to truncated spectrum methods, Rep. Prog. Phys. **81**, 046002 (2018).

[28] A. L. Fitzpatrick and E. Katz, Snowmass white paper: Hamiltonian truncation, arXiv:2201.11696.

[29] Z. Davoudi, I. Raychowdhury, and A. Shaw, Search for efficient formulations for Hamiltonian simulation of non-Abelian lattice gauge theories, Phys. Rev. D **104**, 074505 (2021).

[30] I. D'Andrea, C. W. Bauer, D. M. Grabowska, and M. Freytsis, New basis for Hamiltonian SU(2) simulations, Phys. Rev. D **109**, 074501 (2024).

[31] S. Romiti and C. Urbach, Digitizing lattice gauge theories in the magnetic basis: Reducing the breaking of the fundamental commutation relations, Eur. Phys. J. C **84**, 708 (2024).

[32] T. V. Zache, D. González-Cuadra, and P. Zoller, Quantum and classical spin-network algorithms for q-deformed Kogut-Susskind gauge theories, Phys. Rev. Lett. **131**, 171902 (2023).

[33] G. Bergner, M. Hanada, E. Rinaldi, and A. Schafer, Toward QCD on quantum computer: Orbifold lattice approach, J. High Energy Phys. 05 (2024) 234.

[34] Z. Li, D. M. Grabowska, and M. J. Savage, Sequency hierarchy truncation (SeqHT) for adiabatic state preparation and time evolution in quantum simulations, arXiv:2407.13835.

[35] C. W. Bauer *et al.*, Quantum simulation for high-energy physics, PRX Quantum **4**, 027001 (2023).

[36] L. Funcke, T. Hartung, K. Jansen, and S. Kühn, Review on quantum computing for lattice field theory, Proc. Sci. LATTICE2022 (**2023**) 228 [arXiv:2302.00467].

[37] J. S. Schwinger, Gauge invariance and mass. II., Phys. Rev. **128**, 2425 (1962).

[38] S. R. Coleman, More about the massive Schwinger model, Ann. Phys. (N.Y.) **101**, 239 (1976).

[39] J. Zinn-Justin, *Quantum Field Theory and Critical Phenomena: Fifth Edition* (Oxford University Press, New York, 2021).

[40] H. Ball, M. J. Biercuk, A. R. R. Carvalho, J. Chen, M. Hush, L. A. D. Castro, L. Li, P. J. Liebermann, H. J. Slatyer, C. Edmunds, V. Frey, C. Hempel, and A. Milne, Software tools for quantum control: Improving quantum computer performance through noise and error suppression, Quantum Sci. Technol. **6**, 044011 (2021).

[41] Q-CTRL, Boulder Opal, https://q-ctrl.com/boulder-opal, 2023. [Online].

[42] J. Elias Miro and J. Ingoldby, Effective Hamiltonians and counterterms for Hamiltonian truncation, J. High Energy Phys. 07 (2023) 052.

[43] O. Delouche, J. Elias Miro, and J. Ingoldby, Hamiltonian truncation crafted for UV-divergent QFTs, SciPost Phys. **16**, 105 (2024).

[44] J. Elias-Miro, M. Montull, and M. Riembau, The renormalized Hamiltonian truncation method in the large E_T expansion, J. High Energy Phys. 04 (2016) 144.

[45] T. Cohen, K. Farnsworth, R. Houtz, and M. A. Luty, Hamiltonian truncation effective theory, SciPost Phys. **13**, 011 (2022).

[46] M. K. Lájer and R. M. Konik, Krylov spaces for truncated spectrum methodologies, Phys. Rev. D **109**, 045016 (2024).

[47] T. Banks, L. Susskind, and J. Kogut, Strong-coupling calculations of lattice gauge theories: $(1+1)$-dimensional exercises, Phys. Rev. D **13**, 1043 (1976).

[48] C. J. Hamer, Z. Weihong, and J. Oitmaa, Series expansions for the massive Schwinger model in Hamiltonian lattice theory, Phys. Rev. D **56**, 55 (1997).

[49] C. Hamer, J. Kogut, D. Crewther, and M. Mazzolini, The massive Schwinger model on a lattice: Background field, chiral symmetry and the string tension, Nucl. Phys. **B208**, 413 (1982).

[50] F. Berruto, G. Grignani, G. W. Semenoff, and P. Sodano, Chiral symmetry breaking on the lattice: A study of the strongly coupled lattice Schwinger model, Phys. Rev. D **57**, 5070 (1998).

[51] R. Dempsey, I. R. Klebanov, S. S. Pufu, and B. Zan, Discrete chiral symmetry and mass shift in the lattice Hamiltonian approach to the Schwinger model, Phys. Rev. Res. **4**, 043133 (2022).

[52] M. Bañuls, K. Cichy, J. Cirac, and K. Jansen, The mass spectrum of the Schwinger model with matrix product states, J. High Energy Phys. 11 (2013) 158.

[53] E. Rico, T. Pichler, M. Dalmonte, P. Zoller, and S. Montangero, Tensor networks for lattice gauge theories and atomic quantum simulation, Phys. Rev. Lett. **112**, 201601 (2014).

[54] N. Butt, S. Catterall, Y. Meurice, R. Sakai, and J. Unmuth-Yockey, Tensor network formulation of the massless Schwinger model with staggered fermions, Phys. Rev. D **101**, 094509 (2020).

[55] P. Schmoll, J. Naumann, A. Nietner, J. Eisert, and S. Sotiriadis, Hamiltonian truncation tensor networks for quantum field theories, arXiv:2312.12506.

[56] R. Belyansky, S. Whitsitt, N. Mueller, A. Fahimniya, E. R. Bennewitz, Z. Davoudi, and A. V. Gorshkov, High-energy collision of quarks and mesons in the Schwinger model: From tensor networks to circuit QED, Phys. Rev. Lett. **132**, 091903 (2024).

[57] P. Hauke, D. Marcos, M. Dalmonte, and P. Zoller, Quantum simulation of a lattice Schwinger model in a chain of trapped ions, Phys. Rev. X **3**, 041018 (2013).

[58] N. Klco, E. F. Dumitrescu, A. J. McCaskey, T. D. Morris, R. C. Pooser, M. Sanz, E. Solano, P. Lougovski, and M. J. Savage, Quantum-classical computation of Schwinger model dynamics using quantum computers, Phys. Rev. A **98**, 032331 (2018).

[59] Z. Davoudi, M. Hafezi, C. Monroe, G. Pagano, A. Seif, and A. Shaw, Towards analog quantum simulations of lattice gauge theories with trapped ions, Phys. Rev. Res. **2**, 023015 (2020).
[60] A. F. Shaw, P. Lougovski, J. R. Stryker, and N. Wiebe, Quantum algorithms for simulating the lattice Schwinger model, Quantum **4**, 306 (2020).
[61] N. H. Nguyen, M. C. Tran, Y. Zhu, A. M. Green, C. H. Alderete, Z. Davoudi, and N. M. Linke, Digital quantum simulation of the Schwinger model and symmetry protection with trapped ions, PRX Quantum **3**, 020324 (2022).
[62] R. C. Farrell, M. Illa, A. N. Ciavarella, and M. J. Savage, Scalable circuits for preparing ground states on digital quantum computers: The Schwinger model vacuum on 100 qubits, PRX Quantum **5**, 020315 (2024).
[63] R. C. Farrell, M. Illa, A. N. Ciavarella, and M. J. Savage, Quantum simulations of hadron dynamics in the Schwinger model using 112 qubits, Phys. Rev. D **109**, 114510 (2024).
[64] J. Y. Araz, S. Bhowmick, M. Grau, T. J. McEntire, and F. Ringer, State preparation of lattice field theories using quantum optimal control, arXiv:2407.17556.
[65] H. Bergknoff, Physical particles of the massive Schwinger model, Nucl. Phys. **B122**, 215 (1977).
[66] T. Eller, H. C. Pauli, and S. J. Brodsky, Discretized light cone quantization: The massless and the massive Schwinger model, Phys. Rev. D **35**, 1493 (1987).
[67] C. M. Yung and C. J. Hamer, Discretized light cone quantization of $(1+1)$-dimensional QED reexamined, Phys. Rev. D **44**, 2598 (1991).
[68] N. Anand, A. L. Fitzpatrick, E. Katz, Z. U. Khandker, M. T. Walters, and Y. Xin, Introduction to lightcone conformal truncation: QFT dynamics from CFT data, arXiv:2005.13544.
[69] J. Liu and Y. Xin, Quantum simulation of quantum field theories as quantum chemistry, J. High Energy Phys. 12 (2020) 011.
[70] S. R. Coleman, R. Jackiw, and L. Susskind, Charge shielding and quark confinement in the massive Schwinger model, Ann. Phys. (N.Y.) **93**, 267 (1975).
[71] S. R. Coleman, The quantum Sine-Gordon equation as the massive Thirring model, Phys. Rev. D **11**, 2088 (1975).
[72] J. E. Hetrick and Y. Hosotani, Qed on a circle, Phys. Rev. D **38**, 2621 (1988).
[73] I. Kukuljan, Continuum approach to real time dynamics of $(1+1)$D gauge field theory: Out of horizon correlations of the Schwinger model, Phys. Rev. D **104**, L021702 (2021).
[74] J. L. Cardy, Operator content and modular properties of higher-dimensional conformal field theories, Nucl. Phys. **B366**, 403 (1991).
[75] C. Adam, Massive Schwinger model within mass perturbation theory, Ann. Phys. (N.Y.) **259**, 1 (1997).
[76] M. Lüscher, *On a Relation Between Finite Size Effects and Elastic Scattering Processes* (Springer US, Boston, MA, 1984), pp. 451–472, 10.1007/978-1-4757-0280-4_15.
[77] H. F. Trotter, Approximation of semi-groups of operators, Pac. J. Math. **8**, 887 (1958).
[78] M. Suzuki, Decomposition formulas of exponential operators and Lie exponentials with some applications to quantum mechanics and statistical physics, J. Math. Phys. (N.Y.) **26**, 601 (1985).
[79] A. M. Childs, Y. Su, M. C. Tran, N. Wiebe, and S. Zhu, Theory of trotter error with commutator scaling, Phys. Rev. X **11**, 011020 (2021).
[80] A. H. Al-Mohy and N. J. Higham, A new scaling and squaring algorithm for the matrix exponential, SIAM J. Matrix Anal. Appl. **31**, 970 (2010).
[81] C. R. Harris *et al.*, Array programming with NumPy, Nature (London) **585**, 357 (2020).
[82] A. Javadi-Abhari, M. Treinish, K. Krsulich, C. J. Wood, J. Lishman, J. Gacon, S. Martiel, P. D. Nation, L. S. Bishop, A. W. Cross, B. R. Johnson, and J. M. Gambetta, Quantum computing with Qiskit, arXiv:2405.08810.
[83] A. R. R. Carvalho, H. Ball, M. J. Biercuk, M. R. Hush, and F. Thomsen, Error-robust quantum logic optimization using a cloud quantum computer interface, Phys. Rev. Appl. **15**, 064054 (2021).